Soil Dynamics and Earthquake Engineering 45 (2013) 70–79

Contents lists available at SciVerse ScienceDirect

Soil Dynamics and Earthquake Engineering

journal homepage: www.elsevier.com/locate/soildyn

The dynamics of a pumice granular soil in dry state under isotropic resonant column testing

Kostas Senetakis [a,*], Anastasios Anastasiadis [b], Kyriazis Pitilakis [b], Matthew R. Coop [a]

[a] Department of Civil and Architectural Engineering, City University of Hong Kong, Kowloon Tong, Kowloon, Hong Kong
[b] Department of Civil Engineering, Aristotle University of Thessaloniki, Thessaloniki, Greece

ARTICLE INFO

Article history:
Received 13 August 2012
Received in revised form
21 October 2012
Accepted 22 November 2012
Available online 20 December 2012

ABSTRACT

The response of soils under vibrations strongly depends on the type of particles which reflects the behavior at particle contacts and the micro-mechanisms that dominate granular assemblies. In this paper the dynamic properties of a pumice soil of low bulk density and high porosity were investigated. As a reference soil, a quartzitic crushed rock with hard particles was used. The experiments were performed on dry samples of sand to gravel size under isotropic conditions of confinement in a fixed-free resonant column apparatus. In the range of small strains, the V_s–σ'_m and G_O–σ'_m relationships are dominated by particle type in terms of mineralogy and morphology; plastic response at particle contacts of the pumice samples led to higher n_V and n_G exponents in comparison to the quartz ones. The small-strain damping ratio values were fairly similar for pumice and quartz soils, while the values of the exponent n_D were more scattered. At higher shear strain amplitudes, the pumice soils showed higher linearity in comparison to the quartz ones. This is attributed partially to micro-crushing at particle contacts that occurs during the dynamic loading of the pumice soils which shifts the elastic and volumetric thresholds to higher strains and plays an important role in the energy dissipation in granular assemblies.

1. Introduction

Strong ground motion due to wave propagation and therefore the seismic response of structures and soil–foundation–structure interaction phenomena are strongly correlated to the dynamic properties of soils often expressed in terms of shear modulus, G, and damping ratio, D. The shear modulus is related to the shear wave velocity, V_s, and mass density of the soil, ρ, through Eq. (1), while the damping ratio is defined as the ratio of the energy loss per cycle (ΔW) to the maximum stored energy (W), analytically expressed through Eq. (2) (e.g., [28,13,14,11,16,30]).

$$G = \rho \times V_s^2 \tag{1}$$

$$D = \frac{\Delta W}{2 \times \pi \times W} \tag{2}$$

In the range of very small strains, in general below 10^{-3}% for granular materials, the behavior is approximately linear-elastic. In this range of strains, the shear modulus corresponds to its maximum value, denoted as G_{max} or G_O, and the damping ratio approximates to a minimum value, denoted as D_{min} or D_O. As reported in previous studies (summarized by [31]), non-hysteretic mechanisms can be responsible for wave attenuation phenomena in dry soils at very small strains, such as, for example, thermal relaxation or chemical interactions at contacts. At higher strain levels, the behavior of soils is hysteretic non-linear; the shear modulus decreases while the opposite trend is observed for the damping ratio. Friction at particle contacts and slippage of particles are the main mechanisms that contribute to the energy dissipation and the overall stiffness degradation (e.g., [30]). The linear elastic threshold, denoted as γ_t^e, that expresses the onset of non-linear elastic behavior and the volumetric or cyclic threshold, denoted as γ_t^v or γ_t^c, that expresses the onset of non-linear plastic behavior (e.g., [37,41,8,22,38,16,24]) have been widely used by many researchers in order to study the behavior of soils in distinct ranges.

With reference to uncemented granular soils in a dry state, it has been demonstrated that in addition to the influence of the confining pressure, the stiffness and attenuation parameters strongly depend on particle type in terms of mineralogy and morphology, through the response at particle contacts, the elastic properties of the individual particles and the packing of the granular assembly (e.g., [12,36,10,3,31,32,30,5,4,34]). The packing of particles is usually expressed in terms of a global void ratio, e, and depends on the grain size distribution, the state of confinement, the depositional process for natural soils or the compaction/reconstitution process for laboratory created soils, as well as the shape of particles (e.g., [42,30,24,5,33]).

* Corresponding author. Tel.: +852 34426528.
E-mail address: ksenetak@cityu.edu.hk (K. Senetakis).

0267-7261/$ - see front matter © 2012 Elsevier Ltd. All rights reserved.
http://dx.doi.org/10.1016/j.soildyn.2012.11.009

As theoretically and experimentally demonstrated by Santamarina and Cascante [31] and Cascante and Santamarina [3], the forces developed at particle contacts, the distribution of contacts in the granular assembly and particle orientations describe the "state" of a granular material and comprise the key components that connect the micro-mechanical and the overall macro-mechanical response of particulate media at very small strains. Using the descrete element method in order to study the micro-mechanical behavior of granular assemblies, Radjai et al. [27] demonstrated that the magnitude and distribution of interparticle forces strongly depend on the grading, an observation which has been also supported from a macro-mechanical point of view by experimental studies on granular materials through element testing (e.g., [24,25,40,34]).

The response of soils at shear strains beyond the elastic threshold also depends on particle type. In recent studies by Senetakis [33] and Senetakis et al. [34], who studied the dynamic behavior of quartzitic granular materials and volcanic soils composed of a rhyolitic glassy rock, it was revealed that soils of variable mineralogy and morphology of particles show markedly different macro-scale responses at small to medium strain levels. Senetakis et al. [34] attributed these differences to the different micro-mechanisms that dominate at particle contacts.

This study aims to investigate in the laboratory the dynamic properties of the coarse fractions of a pumice material of low bulk density and high porosity. As a reference soil, the gravel size fractions of a quartz crushed rock of hard particles are used. The experiments were performed in a fixed-free resonant column (RC) device, capable of measuring the dynamic properties of soils from very small to medium shear strain amplitudes. The samples were tested in a dry state under isotropic conditions of confinement. Based on the RC test data, micro-mechanical interpretations are also presented and discussed.

2. Materials, sample preparation and testing program

2.1. Material used

Four granular soils composed of a pumice material of low density and high porosity were examined in this study. The pumice material has a specific gravity of solids, G_s, equal to 2.18 [33]. The coarse fractions of quartz crushed rock of G_s equal to 2.67 were used as reference soils. All the materials were washed on sieve No. 200 (75 μm) in order to remove the fine particles and then oven-dried before the preparation of laboratory samples of specific grading characteristics. The grading curves of the samples and the classification according to [2] specification are given in Table 1 and Fig. 1.

Table 1
Grain-size characteristics and classification of materials used.

Laboratory material	Parent soil	D_{max}[a] (mm)	D_{50}[b] (mm)	C_u[c]	C_c[d]	Gravel[e] (%)	USCS[f]
LWC2D1	Pumice	4.75	1.50	2.33	1.16	0	SP
LWC2D3	Pumice	6.35	3.00	1.55	0.74	1	SP
LWC1D6	Pumice	9.53	5.60	1.20	0.97	96	GP
LWC1D10	Pumice	12.7	9.50	1.45	0.93	100	GP
C1D6	Quartz	6.35	5.50	1.17	0.96	100	GP
C1D8	Quartz	9.53	7.80	1.22	0.94	100	GP
C1D10	Quartz	12.7	10.1	1.03	1.00	100	GP

[a] Maximum grain size.
[b] Mean grain size.
[c] Coefficient of uniformity $C_u = D_{60}/D_{10}$.
[d] Coefficient of curvature $C_c = D_{30}^2/(D_{60} \times D_{10})$.
[e] Gravel content by weight.
[f] ASTM D2487-00.

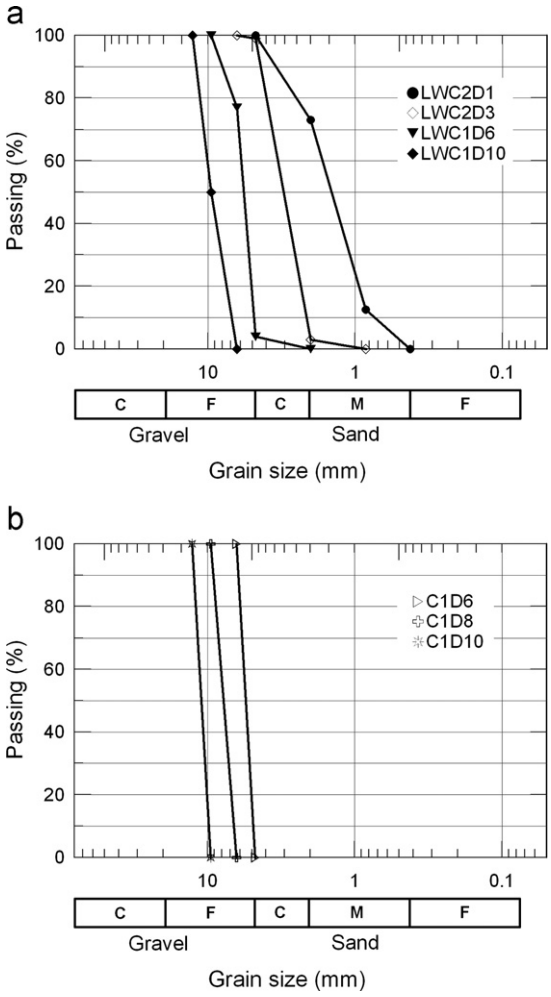

Fig. 1. Grain size distribution curves of materials studied: (a) pumice granular soils (b) quartz gravels.

It is noted that the pumice soils LWC1D6 and LWC1D10 have identical grading curves with the quartz soils C1D6 and C1D10, respectively, while the symbols used to denote the samples reflect the type of soil and the grain size distribution. For example, LWC2D1 corresponds to a pumice soil of $C_u \approx 2$ and $D_{50} \approx 1$ mm, where "LW" denotes lightweight—pumice soil, and C1D6 corresponds to a quartz gravel of $C_u \approx 1$ and $D_{50} \approx 6$ mm. Observing representative particles through a microscope and using empirical diagrams proposed in the literature [21], it was demonstrated that both the pumice and the quartz soils had primarily sub-angular particles.

For the coarse fractions of the pumice soil, the maximum and minimum dry densities ($\gamma_{d,max}$, $\gamma_{d,min}$) range between 6.0–7.5 kN/m^3 and 5.0–6.0 kN/m^3, respectively, and the corresponding minimum and maximum void ratios (e_{min}, e_{max}) range between 1.9–2.5 and 2.5–3.0, approximately [33]. The coarse fractions of the quartz crushed rock have quite typical values of these compaction parameters, of around 14.5–15.5 kN/m^3 and 11.0–12.0 kN/m^3 for the maximum and minimum dry densities, respectively [33]. These differences are attributed to the intra-particle voids of the pumice soil which is related to the geological formation of the parent volcanic rock (e.g., [39]).

2.2. Experimental equipment and sample preparation

All experiments were performed on dry specimens 71 mm in diameter and 142 mm in height in a resonant column (RC)

apparatus of fixed-free type [9] capable of longitudinal and torsional dynamic loading. A description and details of the experimental equipment used have been given elsewhere [33–35]. To summarize, the bottom, passive end of the specimen is rigidly fixed on a base pedestal of mass and inertia that are much higher than those of the specimen, whilst a sinusoidal excitation is applied at the top-active end of the specimen. For this purpose, an excitation mechanism is fixed on the top of the sample, which has two magnets surrounded by four coils for torsional loading, as well as one magnet surrounded by one coil for longitudinal loading. The RC tests are controlled and monitored manually by electronic equipment. Accelerometers, attached to the excitation mechanism and accompanied by amplifiers, are used to record the response at the active end of the sample. The vertical (axial) strains are recorded by a linearly variable differential transformer (LVDT) with a resolution of 0.01 mm.

Samples of the same material were prepared at variable initial void ratios using different preparation methods. Loose specimens were constructed by dry pluviation of the material into a split mold in the RC device. Medium dense and dense to very dense samples were prepared in many layers of equal dry mass and compacted using a metal hammer of diameter approximately half the diameter of the specimen. The preparation methods of dry pluviation and dry compaction in layers are denoted as "DP-M" and "DC-M", respectively.

2.3. Resonant column testing program

After the preparation of the samples and before the set up of the RC apparatus, the specimens were supported through a vacuum of the order of -5 to -10 kPa. At this point the dimensions of the sample were measured and thus, knowing the dry mass of the material used, the initial void ratio (e_o) and dry density (γ_{do}) of the specimens were determined. Low-amplitude torsional resonant column tests (LARCT) were performed at increasing steps of the mean effective confining pressure, σ'_m, between 25 and 400 kPa. In most samples, high-amplitude tests (HARCT) were also performed at least at two levels of the mean effective stress. The isotropic pressure was provided and controlled manually by a pressure board and recorded at the bottom of the triaxial cell by analogue transducer of 1 kPa resolution.

Table 2 summarizes the fifteen specimens tested in the RC apparatus; nine specimens were composed of the coarse fractions of the pumice soil and six specimens were composed of the quartz crushed rock. In agreement with the compaction tests, the specimens of the pumice soil had significantly lower values of the initial dry density (γ_{do}) and higher values of the void ratio (e_o) in comparison to the quartz samples. In general, the LARCT measurements were obtained at shear strain amplitudes in the range 5×10^{-4}–1.0×10^{-3}%. The experiments and the analysis of the RC test results were performed according to the ASTM D4015-92 specification [1].

3. Experimental results and discussion

3.1. Small-strain dynamic properties of pumice and quartz granular soils

3.1.1. Typical LARCT results–empirical relationships used

Typical results of the LARCT program are shown in Figs. 2 and 3, where specimen C1D6-D02 is a quartz gravel and specimen LWC2D1-D12 is a pumice sand. The increase of shear wave velocity, V_s, and small-strain shear modulus, G_O, and the decrease of small-strain damping ratio, D_O, with increasing σ'_m, follow, with a good approximation, a power law. Therefore, the V_s–σ'_m, G_O–σ'_m, and D_O–σ'_m relationships may be expressed through the empirical forms of Eqs. (3)–(5), respectively.

$$V_s = A_V \times (\sigma'_m)^{n_V} \tag{3}$$

$$G_O = A_G \times (\sigma'_m)^{n_G} \tag{4}$$

$$D_O = A_D \times (\sigma'_m)^{n_D} \tag{5}$$

In Figs. 2 and 3, the constants A_V, A_G and A_D, as well as the exponents n_V, n_G and n_D, derived from regression analysis and using Eqs. (3)–(5) are also quoted. Since the parameters V_s and G_O are related to each other through Eq. (1), the exponents n_V and n_G must be related through Eq. (6).

$$n_V = \frac{1}{2} n_G \tag{6}$$

The exponents $n_V(=0.23)$ and $n_G(=0.46)$ of the quartz gravel (Fig. 2) are close to the "typical" values of 0.25 and 0.50, respectively, proposed by many researchers for granular materials ([12,20,43] and others). These values are higher than the theoretical ones (n_G equals 0.33) derived from the assumption of Hertzian contacts and elastic behavior (after [18]), and this is attributed to the plastic deformations that occur at particle contacts during the increase of the confining pressure and the fabric changes in real soils [3].

Table 2
Torsional resonant column testing program.

Code name of specimen	Laboratory material	γ_{do} (kN/m^3)	e_o	Preparation method	σ_m' for HARCT (kPa)
LWC2D1-D01	LWC2D1	7.17	1.981	DC-M*	50,100,200,400
LWC2D1-D11		7.10	1.623	DC-M	50,100
LWC2D1-D12		7.06	2.028	DC-M	–
LWC2D1-D13		5.98	2.575	DP-M**	100,200
LWC2D3-D01	LWC2D3	6.79	2.150	DC-M	100,200
LWC1D6-D01	LWC1D6	6.79	2.153	DC-M	100,200,400
LWC1D6-D12		6.68	2.200	DC-M	–
LWC1D6-D13		6.21	2.445	DP-M	100,200
LWC1D10-D01	LWC1D10	6.45	2.321	DC-M	100,200
C1D6-D01	C1D6	14.0	0.878	DP-M	50,100,200
C1D6-D02		15.4	0.700	DC-M	100,200
C1D8-D01	C1D8	14.2	0.846	DP-M	100,200
C1D8-D02		16.1	0.624	DC-M	50,100
C1D10-D01	C1D10	14.0	0.867	DP-M	50,100
C1D10-D02		16.2	0.618	DC-M	50,100

* Compaction in layers of equal dry mass using a metal hammer in order to prepare medium dense and dense to very dense specimens.
** Dry pluviation in order to prepare loose specimens.

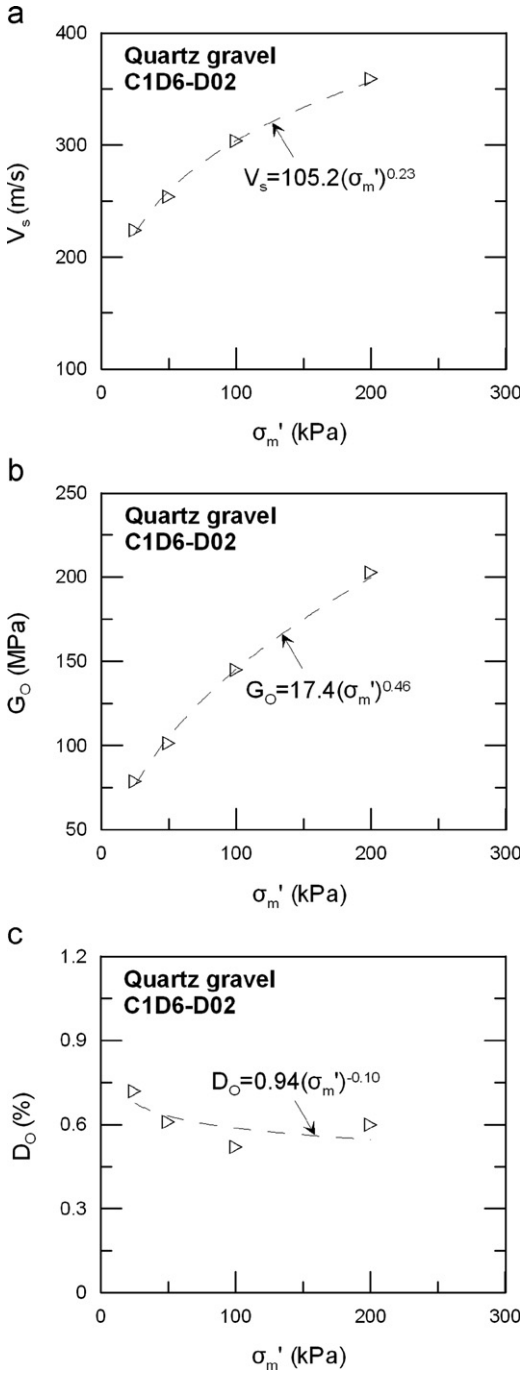

Fig. 2. Effect of mean effective confining pressure on the variation of the small-strain dynamic properties for specimen C1D6-D02 (quartz gravel) and corresponding trend lines.

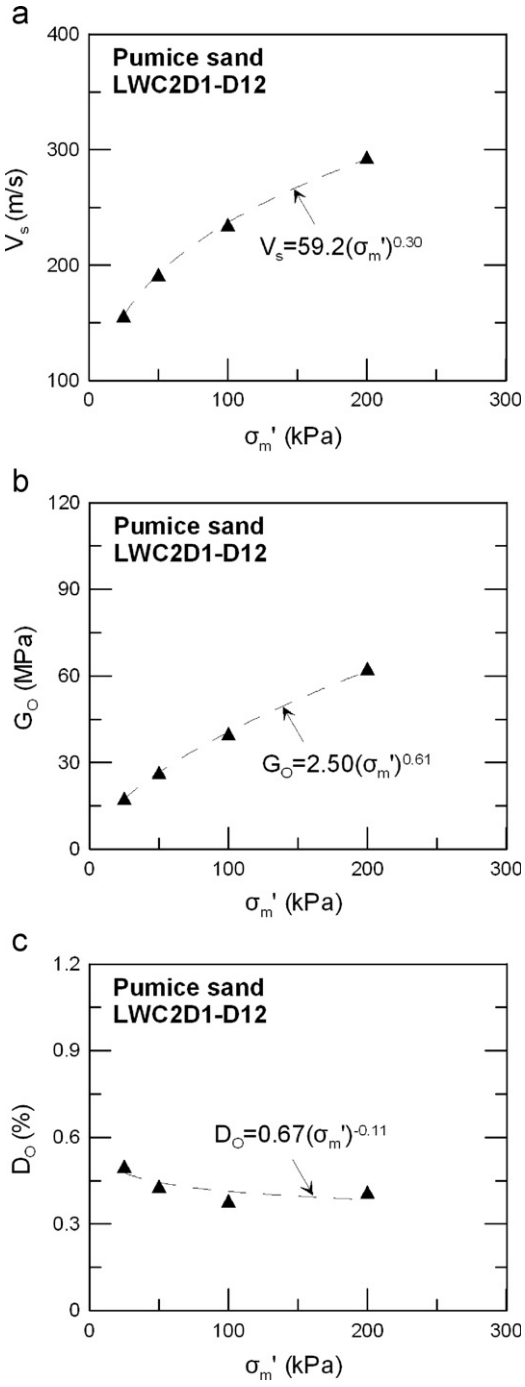

Fig. 3. Effect of mean effective confining pressure on the variation of the small-strain dynamic properties for specimen LWC2D1-D12 (pumice sand) and corresponding trend lines.

The pumice sand of Fig. 3 shows higher values of the exponents n_V and n_G (n_G equals 0.61) which implies that the plastic deformations at the particle contacts of the pumice samples during the increase of the isotropic stress are more pronounced in comparison to the quartz soils. Since materials LWC2D1 and C1D6 have particles of similar roundness, these differences are possibly related, at the micro-scale level, to the effect of particle morphology in terms of surface roughness.

The effect of σ_m' on the small-strain damping ratio is less pronounced than in parameters V_s and G_O, as illustrated in Fig. 2c and 3c. D_O slightly decreases with increasing σ_m' following an exponent n_D of the order of -0.10, which is close to typical values presented in the literature for dry reconstituted granular soils (e.g., [24]). Similarly, Santamarina and Cascante [31] reported that the small-strain damping in granular soils is a function of the isotropic confining pressure, but in that study they reported a higher absolute value of the exponent n_D. Higher absolute values of the exponent n_D were also reported by Senetakis et al. [34] for quartzitic sands and this might be explained by differences in particle shape between the sand-size and gravel-size fractions of the quartz crushed rock used in this study and Senetakis et al. [34] investigation.

The effect of void ratio on the small-strain dynamic properties of representative samples is demonstrated in Fig. 4. V_s and G_O systematically decrease with increasing e. However, the overall

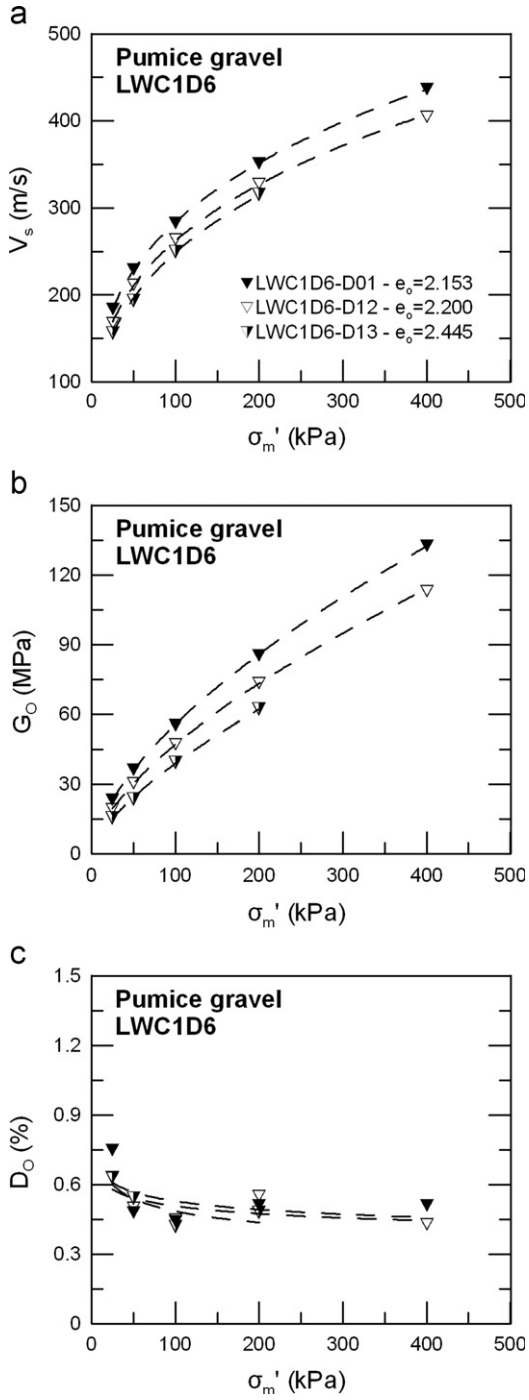

Fig. 4. Effect of void ratio and mean effective confining pressure on the variation of the small-strain dynamic properties for the pumice gravel LWC1D6.

effect of e on D_O is not that strong. This observation was also supported in previous investigations on dry granular soils (e.g., [36], [24,33,34]). Within the framework of this research work, the effect of void ratio on G_O is studied through the general form of Eq. (7) where $F(e)$ is the void ratio function.

$$G_O = A_G^* \times F(e) \times (\sigma_m')^{n_G} \tag{7}$$

The general form of a common void ratio function proposed in the literature is given in Eq. (8).

$$F(e) = \frac{(A-e)^2}{1+e} \tag{8}$$

Hardin and Richart [12] proposed values of the constant A of Eq. (8) equal to 2.17 and 2.97 for granular soils of rounded and angular particles, respectively, while Wichtmann and Triantafyllidis [40] correlated the constant A with the coefficient of uniformity, C_u.

The main shortcoming of the general expression of the void ratio in Eq. (8) is its non-applicability in some types of granular soils, such as soils of high porosity. For example, for threshold void ratio values equal to 2.17 and 2.97, the $F(e)$ function proposed by Hardin and Richart for soils of rounded and angular particles, respectively, becomes zero, and beyond this threshold the trend of decreasing $F(e)$ with increasing e is reversed. Even though void ratio values beyond 1.2 to 1.5 are not the general case of "typical" granular soils, such as quartz sands and gravels of solid particles, the pumice soils have remarkably high e values of the order of 2.0 to 2.6 and thus the effect of void ratio on the stiffness of these materials cannot be expressed effectively through Eq. (8).

Alternatively, an exponential expression of the void ratio function, as shown in Eq. (9) may be more suitable for pumice soils. Jamiolkowski et al. [17] proposed a value of the exponent x_e of Eq. (9) equal to 1.3, Menq [24] correlated the exponent x_e with the mean grain size and in a recent study, Senetakis et al. [34] proposed an expression for the exponent x_e that is a function of the coefficient of uniformity.

$$F(e) = \frac{1}{e^{x_e}} \tag{9}$$

in this study, we adopt the expression of $F(e)$ of Eq. (9) as proposed by Jamiolkowski et al. [17] in order to correlate the small-strain shear modulus with the confining pressure level, and thus Eq. (7) becomes:

$$G_O = A_G^* \times \frac{1}{e^{1.3}} \times (\sigma_m')^{n_G} \tag{10}$$

3.2. Analysis of LARCT results

The analysis of the experimental LARCT results by best-fit of Eqs. (3)–(5) and (10) through the experimental data using regression analysis led to the estimation of the constants A_V, A_G, A_G^*, A_D, n_V, n_G and n_D. All the results stemming from the LARCT data are summarized in Table 3.

Table 3
Small-strain fitting parameters for pumice and quartz soils.

Specimen	V_s–σ_m' relationship		G_O–σ_m' relationship			D_O–σ_m' relationship	
	A_V	n_V	A_G	A_G^*	n_G	A_D	n_D
LWC2D1-D01	62.2	0.30	2.79	6.97	0.60	1.05	−0.12
LWC2D1-D11	66.9	0.29	3.19	6.26	0.59	1.70	−0.33
LWC2D1-D12	59.2	0.30	2.50	6.41	0.61	0.67	−0.11
LWC2D1-D13	44.0	0.35	1.14	4.14	0.71	0.97	−0.13
LWC2D3-D01	55.3	0.34	2.09	6.25	0.68	0.53	−0.03
LWC1D6-D01	67.6	0.31	3.12	8.62	0.63	0.85	−0.11
LWC1D6-D12	60.7	0.32	2.48	7.12	0.64	0.79	−0.10
LWC1D6-D13	51.8	0.34	1.72	5.49	0.68	0.99	−0.15
LWC1D10-D01	81.3	0.28	4.34	11.9	0.56	0.60	−0.02
C1D6-D01	83.4	0.25	9.87	8.41	0.50	1.34	−0.18
C1D6-D02	105.2	0.23	17.4	11.0	0.46	0.94	−0.10
C1D8-D01	76.6	0.27	8.52	6.91	0.53	1.52	−0.16
C1D8-D02	112.3	0.23	20.7	11.3	0.46	1.78	−0.19
C1D10-D01	89.1	0.24	11.1	10.4	0.49	2.66	−0.27
C1D10-D02	100.4	0.24	16.6	5.97	0.48	1.65	−0.26

For the pumice soils, the exponent n_G ranges between 0.56 and 0.71 with an average value of 0.63. For the quartz gravels the values of the exponent n_G are systematically lower than the pumice soils, ranging between 0.46 and 0.53 with an average value of 0.49. The values of the exponent n_D are more scattered in both the pumice and the quartz soils in comparison to the exponents n_V and n_G, ranging from -0.02 to -0.33, but no significant effect of particle type can be noticed. For quartzitic sands of sub-angular to angular particles, Senetakis et al. [34] reported values of the exponent n_G higher than the quartz gravels of this study, ranging between 0.53 and 0.71 with an average value of 0.63.

3.3. The role of particle morphology and initial void ratio in the evolution of axial strains with isotropic compression

The micro-mechanical considerations discussed above relative to the possible role of the behavior at particle contacts and the overall effect of particle morphology in terms of surface roughness on the $V_s-\sigma'_m$ and $G_O-\sigma'_m$ relationships is further supported by the data presented in Fig. 5, where the vertical (axial) strains against σ'_m of representative samples are plotted. For the quartzitic samples C1D6-D01 and C1D6-D02 the axial strains that occurred during the increase of the isotropic stress were small, ranging from values less than 0.1% at $\sigma'_m=25$ kPa to about 0.3% at $\sigma'_m=200$ kPa and consequently the decrease of void ratio with increasing σ'_m was also small. For the pumice soils the axial strains are of about one order of magnitude higher in comparison to the corresponding strains in the quartz soils, which mirrors the more pronounced plastic deformations at particle contacts in the pumice soils and overall the higher values of the exponents n_V and n_G. Fig. 5 also demonstrates the important effect of the initial void ratio on the development of plastic deformations in the pumice samples LWC2D1-D12 and LWC2D1-D13. Even though the vertical strains as presented in this figure are a combination of elastic and plastic response, a reduction of the isotropic stress in some samples after the completion of the RC tests showed that most of the axial strains during the isotropic compression were of plastic nature.

Increasing the initial void ratio at which specimens were prepared in the RC apparatus, which implies a more loose packing of the granular assembly, it is demonstrated in Fig. 5 that the axial strains increase and thus, the permanent changes in fabric due to the isotropic compression are more pronounced as the initial void ratio increases. This is further supported by the results presented in Table 3; for a given sample, the exponents n_V and n_G increase slightly with increasing initial void ratio.

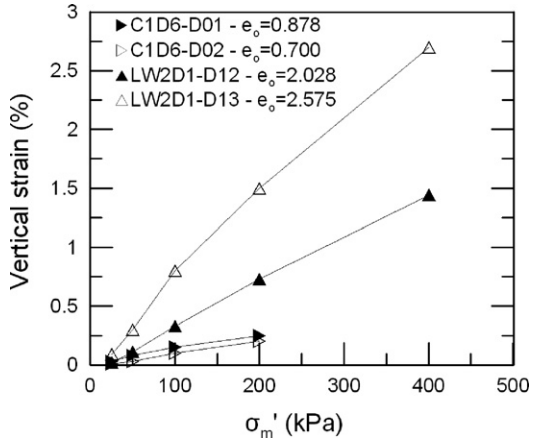

Fig. 5. Evolution of the vertical (axial) strain with increasing mean effective confining pressure in representative specimens.

3.4. Strain-dependent dynamic properties of pumice and quartz granular soils

3.4.1. Typical HARCT results and micromechanical considerations

The variation of the normalized shear modulus, G/G_O, and the damping ratio, D, with increasing shear strain amplitude, γ, for variable values of the mean effective stress, σ'_m, of representative samples is given in Figs. 6 and 7. The increase of γ leads to a reduction in G/G_O and increase in D, but, as illustrated in Figs. 6 and 7, at a given γ, the specimens show a more linear behavior, that is a higher G/G_O and a lower D with increasing σ'_m. In these figures the upper and lower bounds of the G/G_O-logγ and D-logγ curves proposed by Rollins et al. [29] for granular soils are also plotted for comparison.

The curves proposed by Rollins et al. describe satisfactorily the response of the quartz gravel C1D10-D02 (Fig. 7) in the range of small-to-medium strains. However, it is noticeable that the HARCT data of the pumice soil LWC2D1-D01 (Fig. 6) all plot outside of the literature curves, with a remarkably more linear response of the pumice sample in comparison to the corresponding behavior of quartzitic soils; this trend was observed in all the pumice soils. Senetakis [33] also reported a unsatisfactory description of the behavior of other volcanic soils by curves and empirical equations proposed in the literature on the basis of quartzitic soils. In a recent study by Orense et al. [26] it was also

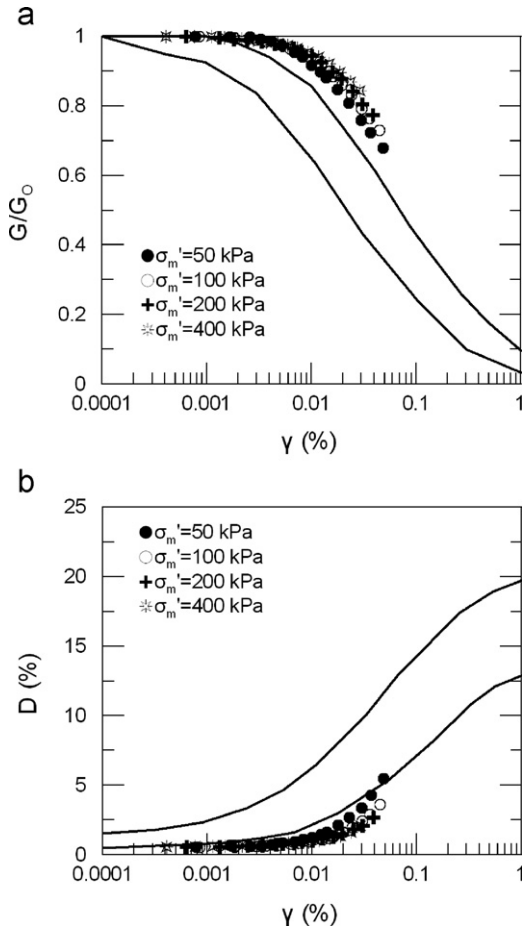

Fig. 6. Effect of shear strain amplitude and confinement on the normalized shear modulus and damping ratio of the pumice sand LWC2D1-D01 (theoretical curves: [29]).

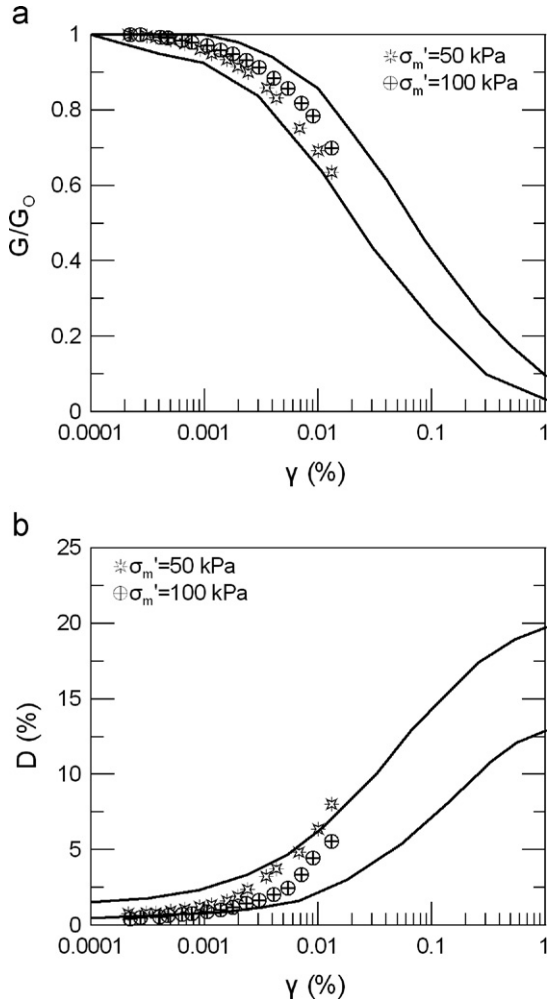

Fig. 7. Effect of shear strain amplitude and confinement on the normalized shear modulus and damping ratio of the quartz gravel C1D10-D02 (theoretical curves: [29]).

revealed that at a given confining pressure level, reconstituted pumice sands exhibit more linear shape of the G/G_O-logγ and D-logγ curves in comparison to quartzitic soils. Similar observations were reported previously by Marks et al. [23].

Beyond the elastic threshold strain, γ_t^e, friction at particle contacts and particle rearrangement dominate the behavior of the granular assembly. These mechanisms contribute to the dissipation of energy, the reduction of shear stiffness and increase in damping. For the pumice soils, the elastic threshold is shifted to higher strain levels in comparison to the quartz gravels. For shear strain amplitudes in the vicinity of 10^{-2}%, which is the typical threshold between non-linear elastic and non-linear plastic behavior (e.g., [37,41,38], Hsu and Vucetic, [15]), in specimen C1D10-D02 a significant reduction of the shear modulus ($G \approx 0.70–0.75 \times G_O$) and increase of the damping ratio ($D \approx 5–6\%$) has occurred (Fig. 7). For the pumice sample LWC2D1-D01 (Fig. 6), the reduction of shear modulus and increase in damping is noticeably less pronounced ($G \approx 0.90–0.94 \times G_O$, $D \approx 1.0–1.5\%$) and that implies a shift of the volumetric threshold, γ_t^v, to higher strain levels for the pumice sand in comparison to the quartzitic soil.

The more linear response of the pumice soil cannot be simply explained by macro-scale considerations, such as the effect of the number of loading cycles or the frequency of loading since the soils of this research work were studied in a dry state and the applied shear strains are, in general, in the range of the non-linear elastic response of the materials. It may then be assumed that other mechanisms dominate the response of the pumice soils in the range of medium strain levels. It is possible that micro-crushing at the asperities of the particles prevails during the cyclic loading, a micro-mechanism which prevents significant particle rearrangement and thus the reduction of shear stiffness and increase in damping is less pronounced in these soils.

In the majority of the quartz samples and for the range of shear strain amplitudes studied, there was observed a small decrease of specimen height during the cyclic loading, in particular for strain levels beyond 10^{-2}%, an observation which implies that plastic deformations occur during the torsional loading of the samples. This was also supported by a small decrease in the initial shear modulus of the quartz soils after the performance of the HARCT. For the pumice soils, no changes of the vertical LVDT readings occurred during the cyclic loading, and the initial shear modulus before and after the performance of the HARCT was found constant.

Visual observation of the individual particles of the pumice soils after the performance of the RC tests as well as sieving analyzes tests of representative samples, did not show any significant damage to the particles or significant shift of the grading curves of the samples before and after the tests. However, it was noticed through visual observation of the samples that finer particles were present in the pumice samples after the RC tests, which demonstrates that damage to the asperities at a micro-scale level has taken place. This micro-crushing could be the result of a coupled effect of the isotropic compression and the cyclic loading at medium strain levels.

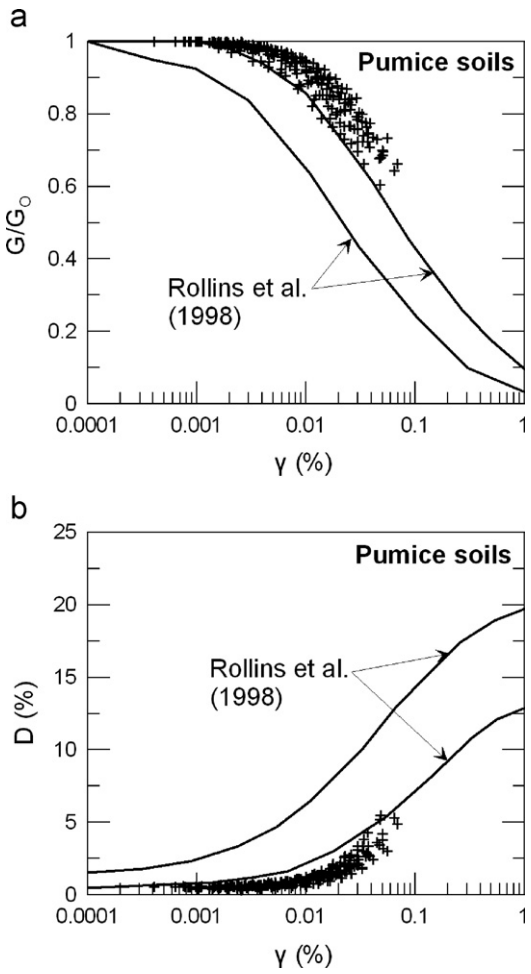

Fig. 8. Summary of the HARCT data for the pumice soils.

3.4.2. Synopsis of HARCT results and analytical models

In Figs. 8 and 9 the HARCT data of all specimens are summarized. As also demonstrated in Fig. 7, the G/G_O-logγ and D-logγ curves proposed by Rollins et al. [29] describe satisfactorily the response of the quartz soils (Fig. 9), whereas in Fig. 8 it is evident that the pumice granular soils show a significantly more linear response in comparison to the quartzitic soils.

For the extrapolation of the HARCT data to higher strain levels as well as for the analytical correlation between the normalized shear modulus and damping ratio with the shear strain amplitude, commonly used models and equations of empirical form, proposed in the literature, are utilized herein. In particular, a modification of the hyperbolic model as proposed by Darendeli [6,7] was used for the correlation between G/G_O and γ. The damping ratio, expressed as D–D_O, was correlated to the normalized shear modulus, through a second order polynomial equation.

The analytical expression of the modified hyperbolic model is given in Eq. (11), where γ_{ref} is the reference strain that expresses the "linearity", and parameter (a), namely the coefficient of curvature, expresses the overall slope of the G/G_O-logγ curve [6,7,24]. Parameter (a) was introduced by Darendeli [6,7] for a best-fit of the hyperbolic model to the experimental data since, initially, in the hyperbolic model proposed by Hardin and Drnevich [13,14], the only fitting parameter was the reference strain.

$$\frac{G}{G_O} = \frac{1}{1+\left(\frac{\gamma}{\gamma_{ref}}\right)^a} \tag{11}$$

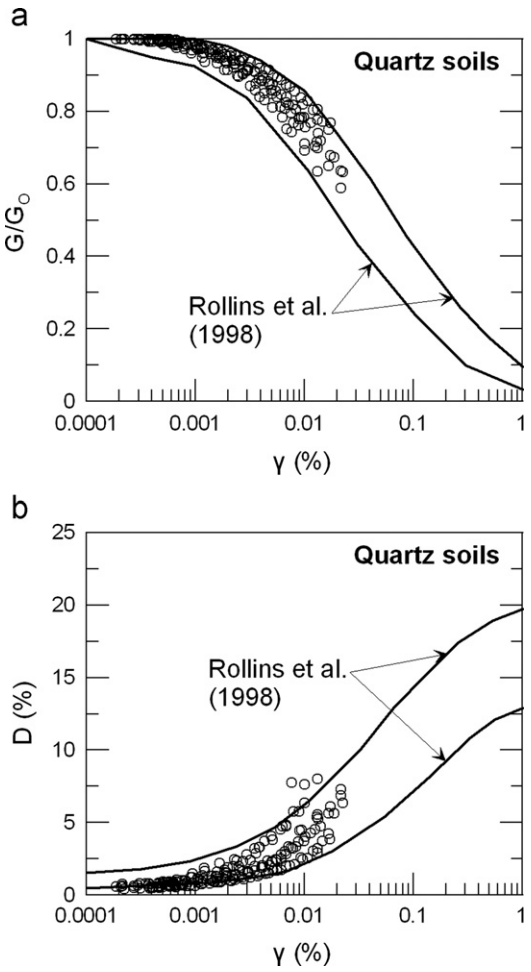

Fig. 9. Summary of the HARCT data for the quartz soils.

For granular soils in a dry state, γ_{ref} strongly depends on the confining pressure level and the coefficient of uniformity (e.g., [24,33]); γ_{ref} increases with increasing σ'_m and decreasing C_u. In this study, the reference strain is expressed analytically through the empirical form of Eq. (12), where A_γ is a constant that primarily depends on soil type and grading and n_γ is an exponent that expresses the effect of σ'_m on the reference strain. This equation in its general form was previously proposed by Menq [24] for granular soils and Zhang et al. [44] for soils of variable geologic age.

$$\gamma_{ref} = A_\gamma \times (\sigma'_m)^{n_\gamma} \tag{12}$$

The damping ratio was correlated with the normalized shear modulus through Eq. (13), where a_1, a_2 and a_3 are constants and D_O is the small-strain damping ratio. This equation in its general form was previously proposed by Zhang et al. [44].

$$D-D_O(\%) = a_1 \times \left(\frac{G}{G_O}\right)^2 + a_2 \times \left(\frac{G}{G_O}\right) + a_3 \tag{13}$$

3.4.3. Analysis of HARCT results

Using the modified hyperbolic model, the reference strain and coefficient of curvature of all specimens at variable mean effective stresses were evaluated by fitting of the analytical model of Eq. (11) to the experimental data. The fitting parameters A_γ and n_γ were then determined by plotting the reference strain against σ'_m. These parameters as well the values of the coefficient of curvature (a) are summarized in Table 4 for all the pumice and the quartz soils.

There was no clear trend observed for the effect of σ'_m or C_u on the fitting parameter (a). For the pumice soils, (a) ranges between 0.96 and 1.18 with an average value of 1.12 and a standard deviation equal to 0.06. For the quartz soils, parameter (a) is systematically lower, ranging between 0.95 and 1.08, with an average value equal to 1.00 and a standard deviation of 0.04. The higher (a) values of the pumice soils imply that the rate of G/G_O decrease, below a threshold strain that corresponds to G/G_O=0.50, is less pronounced in comparison to the quartz soils. However, for higher strain levels, the rate of stiffness degradation in the pumice soils becomes more pronounced and that mirrors a threshold, where suddenly significant slippage at particle contacts and rearrangement of the particles occur.

As shown in Table 4, the values of the exponent n_γ are scattered. For the pumice soils the average n_γ is equal to 0.25, and for the quartz gravels the corresponding average value is equal to 0.47, and that implies a less pronounced effect of σ'_m on

Table 4
Non-linear fitting parameters for pumice and quartz soils.

Code name of specimen	$A_{\gamma,ref}$ (%)	$n_{\gamma,ref}$	(a) values at variable σ'_m (kPa)			
			50	100	200	400
LWC2D1-D01	5.3×10^{-2}	0.15	1.10	1.14	1.14	1.16
LWC2D1-D11	7.6×10^{-2}	0.07	1.18	1.16	–	–
LWC2D1-D13	1.6×10^{-2}	0.42	–	1.16	1.10	–
LWC2D3-D01	2.2×10^{-2}	0.27	–	1.10	1.10	–
LWC1D6-D01	[a]	[a]	–	[a]	[a]	–
LWC2D1-D13	[a]	[a]	–	[a]	[a]	–
LWC1D10-D01	1.3×10^{-2}	0.34		1.10	0.96	–
C1D6-D01	7.6×10^{-3}	0.36	0.95	0.99	0.97	–
C1D6-D02	1.3×10^{-2}	0.26	–	0.97	0.99	–
C1D8-D01	1.9×10^{-3}	0.66	–	1.04	1.03	–
C1D8-D02	2.3×10^{-3}	0.56	0.98	0.96	–	–
C1D10-D01	3.0×10^{-3}	0.47	1.08	1.00	–	–
C1D10-D02	3.8×10^{-3}	0.52	0.98	1.00	–	–

[a] Not included.

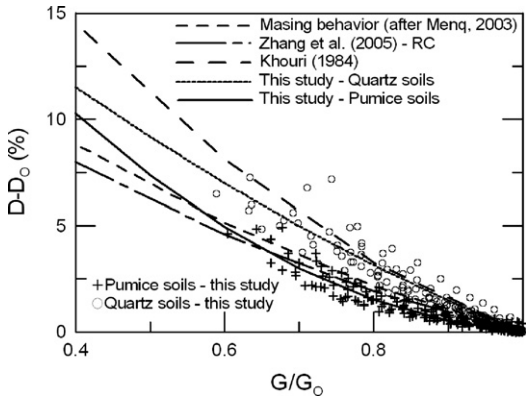

Fig. 10. Correlation between the increase in damping and decrease in shear stiffness of the pumice and the quartz soils of this study in comparison to theoretical curves proposed in the literature.

the G/G_O-logγ curves of the pumice soils in comparison to the quartzitic granular materials. Similarly, Senetakis [33] reported a less pronounced effect of the confinement level on the non-linear response of other volcanic soils in comparison to quartz sands.

Regarding the constant A_γ, it can be seen in Table 4 that the pumice soils exhibit systematically higher values in comparison to the quartz ones, a trend which supports the observations from Figs. 6–9 that the pumice soils exhibit a significantly more linear shape of the G/G_O-logγ curves and that in these soils there is a shift of the elastic and volumetric thresholds to higher strains.

The correlation between the stiffness degradation and the increase in damping is shown in Fig. 10. In the same figure trend lines of polynomial form are shown for the pumice and quartz soils as well as correlations presented in the literature [19,24,44]. Through regression analysis and using Eq. (13), the fitting parameters a_1, a_2 and a_3 were evaluated as 23.7, −50.3 and 26.6 for the pumice soils, and 8.5, −31.1 and 22.6 for the quartz gravels, respectively.

3.4.4. Proposed relationships and design G/G_O-logγ and D-logγ curves

Following the analysis of the HARCT data presented above, the expressions for the estimation of the stiffness degradation and increase in damping with increasing shear strain amplitude, are summarized below, separately for pumice soils of sand to gravel size and uniform quartz soils of gravel size. In these equations, σ'_m is given in kPa, while γ, γ_{ref}, and the damping ratio are given in percentile scale. The values of 3.60×10^{-2} in Eq. (15) and 5.27×10^{-3} in Eq. (18) correspond to the average $A\gamma$(%) values as determined from the results presented in Table 4.

Granular pumice soils:

$$\frac{G}{G_O}=\frac{1}{1+\left(\frac{\gamma}{\gamma_{ref}}\right)^{1.12}} \tag{14}$$

$$\gamma_{ref}(\%)=3.60\times10^{-2}\times\left(\sigma'_m\right)^{0.25} \tag{15}$$

$$D-D_O(\%)=23.7\times\left(\frac{G}{G_O}\right)^2-50.3\times\left(\frac{G}{G_O}\right)+26.6 \tag{16}$$

Uniform quartz gravels:

$$\frac{G}{G_O}=\frac{1}{1+\left(\frac{\gamma}{\gamma_{ref}}\right)} \tag{17}$$

$$\gamma_{ref}(\%)=5.27\times10^{-3}\times\left(\sigma'_m\right)^{0.47} \tag{18}$$

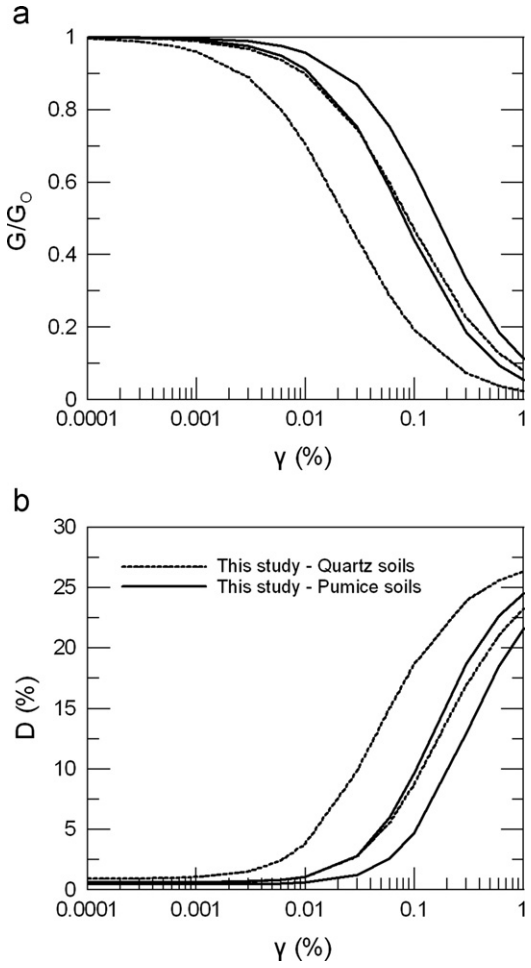

Fig. 11. Design normalized shear modulus reduction and damping ratio increase curves of this study for pumice and quartz soils corresponding to σ_m' equal to 25 and 400 kPa.

$$D-D_O(\%)=8.5\times\left(\frac{G}{G_O}\right)^2-31.1\times\left(\frac{G}{G_O}\right)+22.6 \tag{19}$$

Based on the results stemming from the HARCT program of this study and using Eqs. (14)–(19), design G/G_O-logγ and D-logγ curves for pumice and quartz coarse grained soils are plotted in Fig. 11. These curves correspond to σ'_m values equal to 25 and 400 kPa. As also mentioned previously, the overall effect of the confining pressure is less pronounced in the pumice soils, and thus the increase of σ'_m leads to a less pronounced shift of the curves of Fig. 11 for the pumice soils in comparison to the quartz ones. The higher coefficient of curvature (a) that the pumice soils exhibit reflects the slightly steeper slope of the G/G_O-logγ and D-logγ curves for these materials at high strain levels ($>10^{-2}$%).

4. Conclusions

In this study the coarse fractions of a pumice soil of low density and high porosity were examined in a dry state under isotropic torsional resonant column testing. The gravel size fractions of a quartz crushed rock were used as reference soils.

In the range of very small strains, the pumice samples showed significantly lower shear moduli in comparison to the quartz ones; this is attributed to the higher void ratio and lower dry density of the pumice samples. However, attenuation parameters were fairly similar between pumice and quartzitic specimens. The V_s–σ'_m and G_O–σ'_m relationships strongly depend on the behavior

at particle contacts and thus on the type of particles which includes both mineralogy and morphology. For the pumice soils, the analysis of the RC data demonstrated higher n_V and n_G values in comparison to the quartz samples, which is related to plastic deformations at particle contacts during the increase of the isotropic stress. The D_O–σ'_m relationship was less affected by particle type, while the n_D values were more scattered.

In the range of medium strain levels, it was revealed that the pumice soils exhibit a more linear shape of the G/G_O-logγ and D-logγ curves in comparison to the quartz ones, with a shift of the elastic and volumetric thresholds to higher strains. These observations are attributed partially to micro-crushing of the asperities at the contacts of the pumice particles which would play an important role on the energy dissipation. Based on commonly used analytical models and equations of empirical form and after modifying the various constants, appropriate relationships were proposed for the estimation of the shear modulus and damping ratio of pumice and quartz gravels over a wide range of shear strain amplitudes.

Acknowledgments

The authors would like to thank the anonymous reviewers for their constructive comments and their detailed suggestions which helped us to improve the quality of the paper. The first author was supported by the Research Project 83357 entitled "Seismic Engineering Research Infrastructures For European Synergies (SERIES)" funded by the EUROPEAN COMMISSION during the performance of the laboratory tests, the Strategic Research Grant 7002667 entitled "The development of a new soil particle loading apparatus" and the Start-Up Research Grant 9380056 entitled "Experimental soil mechanics" funded by the City University of Hong Kong during the preparation of the paper.

References

[1] ASTM. Standard test methods for modulus and damping of soils by the resonant column method: D4015-92. Annual Book of ASTM Standards, ASTM International 1992.
[2] ASTM. Standard practice for classification of soils for engineering purposes (Unified Soil Classification System): D2487-00. Annual Book of ASTM Standards, ASTM International (2000).
[3] Cascante G, Santamarina C. Interparticle contact behavior and wave propagation. Journal of Geotechnical and Geoenvironmental Engineering, ASCE 1996;122(10):831–9.
[4] Clayton C. Stiffness at small strain: research and practice. Géotechnique 2011;61(1):5–37.
[5] Cho G-C, Dodds J, Santamarina C. Particle shape on packing density, stiffness, and strength. Journal of Geotechnical and Geoenvironmental Engineering, ASCE 2006;132(5):591–602.
[6] Darendeli M. Dynamic properties of soils subjected to 1994 Northridge earthquake. MS dissertation. University of Texas at Austin, USA, 1997.
[7] Darendeli M. Development of a new family of normalized modulus reduction and material damping curves. PhD dissertation. University of Texas at Austin, USA, 2001.
[8] Dobry R, Ladd R, Yokel F, Chung R Powell D. Prediction of pore water pressure buildup and liquefaction of sands during earthquakes by the cyclic strain method. National Bureau of Standards Building Science Series 138, National Bureau of Standards and Technology: Gaithersburg, Md.; 1501982.
[9] Drnevich V.. Effects of strain history on the dynamic properties of sand. PhD dissertation. University of Michigan, USA, 1967.
[10] Edil T Luh G. Dynamic modulus and damping relationships for sands. Proceedings, geotechnical division speciality conference on earthquake engineering and soil dynamics. ASCE: Pasadena, CA.; Vol.1. 1978 p. 394–409.
[11] Gazetas G., Foundation vibrations, foundation engineering handbook, Fang HY and Van Nostrand Reinhold (editors.): NY; USA. p.553–593, 1991.
[12] Hardin B, Richart F. Elastic wave velocities in granural soils. Journal of the Soil Mechanics and Foundations Division, ASCE 1963;89(SM1):33–65.
[13] Hardin B, Drnevich V. Shear modulus and damping in soils: measurement and parameter effects. Journal of the Soil Mechanics and Foundations Division, ASCE 1972;18(6):603–24.
[14] Hardin B, Drnevich V. Shear modulus and damping in soils: design equations and curves. Journal of the Soil Mechanics and Foundations Division, ASCE 1972;98(7):667–92.
[15] Hsu C-C, Vucetic M. Volumetric threshold shear strain for cyclic settlement. Journal of Geotechnical and Geoenvironmental Engineering, ASCE 2004;130(1):58–70.
[16] Ishihara K. Soil behaviour in earthquake geotechnics. Oxford Science Publications; 1996.
[17] Jamiolkowski M, Leroueil S and Lo Priesti D., (1991). Design parameters from theory to practice. Proceedings, international conference on geotechnical engineering for coastal development: geo-coast 1991, coastal development institute of technology. Yokohama, Japan. p.877–91.
[18] Johnson KL. Contact mechanics. Cambridge: Cambridge University Press; 1985.
[19] Khouri N. Dynamic properties of soils. MS dissertation. Department of civil engineering; Syracuse University1984.
[20] Kokusho T. Cyclic triaxial test of dynamic soil properties for wide strain range. Soils and Foundations 1980;20(2):45–60.
[21] Krumbein W, Sloss L. Stratigraphy and sedimentation. San Francisco: W.H. Freeman and Company; 1963.
[22] Ladd R, Dobry R, Dutko P, Yokel F, Chung R. Pore-water pressure buildup in clean sands because of cyclic straining. Geotechnical Testing Journal 1989;12(1):77–86.
[23] Marks S, Larkin T, Pender M. The dynamic properties of a pumiceous sand. Bulletin of the New Zealand National Society for Earthquake Engineering 1998;31(2):86–102.
[24] Menq F-Y. Dynamic properties of sandy and gravelly soils. PhD dissertation. University of Texas at Austin, USA, 2003.
[25] Menq F-Y and Stokoe K. Linear dynamic properties of sandy and gravelly soils from large-scale resonant tests, deformation characteristics of geomaterials, H Di Benedetto, T Doanh, H Geoffroy and C Sauzeat (editors.): Swets & Zeitlinger, Lisse. p. 63–712003.
[26] Orense R, Hyodo M, Kaneko T. Dynamic deformation characteristics of pumice sand, New Zealand society for earthquake engineering (2012 NZSEE) conference. University of Canterbury; Christchurch, NZ, 2012.
[27] Radjai F, Wolf D, Jean M, Moreau J-J. Bimodal character of stress transmission in granular packing. Physical Review Letters 1998;80(1):61–4.
[28] Richart F, Woods R, Hall J. Vibrations of soils and foundations. Englewood Cliffs, New Jersey, USA: Prentice-Hall, Inc.; 1970.
[29] Rollins K, Evans M, Diehl N, Daily W. Shear modulus and damping relationships for gravels. Journal of Geotechnical and Environmental Engineering 1998;124(5):396–405.
[30] Santamarina C, Klein K, Fam M. Soils and waves. New York, USA: John Wiley and Sons; 2001.
[31] Santamarina C, Cascante G. Stress anisotropy and wave propagation: A micromechanical view. Canadian Geotechnical Journal 1996;33:770–82.
[32] Santamarina J, Cascante G. Effect of surface roughness on wave propagation parameters. Geotechnique 1998;48(1):129–37.
[33] Senetakis K. Dynamic properties of granular soils and mixtures of typical sands and gravels with recycled synthetic materials. PhD dissertation. Department of civil engineering: Aristotle University of Thessaloniki; Greece (in Greek),2011.
[34] Senetakis K, Anastasiadis A, Pitilakis K. The small-strain shear modulus and damping ratio of quartz and volcanic sands. Geotechnical Testing Journal 2012;35(6) (ISSN: 1945–7545).
[35] Senetakis K, Anastasiadis A, Pitilakis K. Dynamic properties of dry sand/rubber (RSM) and gravel/rubber (GRM) mixtures in a wide range of shearing strain amplitudes. Soil Dynamics and Earthquake Engineering 2012;33:38–53.
[36] Sherif M, Ishibashi I, Gaddah A. Damping ratio for dry sands. Journal of Geotechnical Engineering, ASCE 1977;103(7):743–56.
[37] Silver M, Seed H. Volume changes in sands during cyclic loading. Journal of Soil Mechanics and Foundations, ASCE 1971;97(9):1171–82.
[38] Vucetic M. Cyclic threshold shear strains in soils. Journal of Geotechnical Engineering, ASCE 1994;120(12):2208–28.
[39] Wesley L.D., (). Chapter 21—geotechnical characteristics of a pumice sand. Proceedings of the second international workshop on characterization and engineering properties of natural soils, KK Phoon, DW Hight, S Leroueil and TS Tan (editors.); Singapore, 2006.
[40] Wichtmann T, Triantafyllidis Th. Influence of the grain-size distribution curve of quartz sand on the small strain shear modulus G_{max}. Journal of Geotechnical and Geoenvironmental Engineering, ASCE 2009;135(10):1404–18.
[41] Youd LT. Compaction of sands by repeated shear straining. Journal of Soil Mechanics and Foundations, ASCE 1972;98(7):709–25.
[42] Youd T., (1973). Factors controlling the maximum and minimum densities of sands, evaluation of relatice density and its role in geotechnical projects involving cohesionless soils, ASTM, special technical publication 523. American society for testing and materials: Philadelphia, USA; p. 98–112.
[43] Yu P, Richart F. Stress ratio effects on shear modulus of dry sands. Journal of Geotechnical Engineering, ASCE 1984;110(3):331–45.
[44] Zhang J, Andrus R, Juang C. Normalized shear modulus and material damping ratio relationships. Journal of Geotechnical and Geoenvironmental Engineering, ASCE 2005;131(4):453–64.